Monocrystal Elastic Constants of the Negative-Thermal-Expansion Compound Zirconium Tungstate (ZrW_2O_8)

F. R. Drymiotis, H. Ledbetter, J. B. Betts, T. Kimura, J. C. Lashley, and A. Migliori
Los Alamos National Laboratory, Los Alamos, New Mexico 87545, USA

A. Ramirez and G. Kowach
Lucent Technologies/Bell Laboratories, Murray Hill, New Jersey 07974, USA

J. Van Duijn
Johns Hopkins University, Baltimore, Maryland 21218, USA
(Received 26 January 2004; published 8 July 2004)

We measured zirconium tungstate's elastic constants C_{ij}. This compound shows relatively soft, nearly isotropic elastic constants with normal Poisson ratios and no approach to Born instability. ZrW_2O_8 shows normal ambient-temperature elastic constants C_{ij}, but remarkable dC_{ij}/dT that show dominant low-frequency acoustic-vibration modes. From the bulk modulus, we estimated the total ambient-temperature thermodynamic Grüneisen parameter as $\gamma = -1.2$. The dB/dT slope gives a Grüneisen parameter $\gamma = -7$. The 300–0 K bulk-modulus increase (40%) seems unprecedented and breaks Birch's law of corresponding states.

DOI: 10.1103/PhysRevLett.93.025502 PACS numbers: 62.20.Dc

Since the discovery in 1968 that zirconium-tungstate contracts when heated [1], much research ensued, both measurements and theories [2–7]. Zirconium tungstate represents perhaps the paradigm negative-thermal-expansion material: cubic crystal structure (thus, isotropic contraction), continued shrinking when heated over a wide temperature range (0–1050 K), a nearly constant thermal-expansivity coefficient $\beta = (1/V)(dV/dT)_P$, and (for oxides) large β.

Negative thermal expansion is attributed to lattice geometry: a large (44-atom) unit cell, interconnected Zr-O octahedra and W-O tetrahedra [8]. Zirconium tungstate's elastic constants C_{ij} assume importance for several reasons: (i) The C_{ij} reflect interatomic bonds, thus a check on interatomic potentials and assumptions about ionicity covalency. (ii) The bulk modulus $B = (C_{11} + 2C_{12})/3$ by high-pressure neutron diffraction [9] differs enormously from a theoretical estimate [10]. (iii) Some studies conclude that negative thermal expansion of a network structure implies a negative Poisson ratio [6]. (iv) Reported Debye or Einstein temperatures vary widely, and the C_{ij} provide a good estimate of these. (v) An accurate bulk modulus B gives a good estimate of the total thermodynamic Grüneisen parameter. (vi) The C_{ij} provide a check on neutron-diffraction Born–von Karman force constants. (vii) From the C_{ij}, we can see whether any of the Born stability criteria accompany negative thermal expansion. (viii) The elastic-constant temperature derivatives dC_{ij}/dT relate directly to the Grüneisen parameter and to the equation of state.

Monocrystals were made using a nonequilibrium technique described elsewhere [2]. The specimen consisted of a (100)-oriented rectangular parallelepiped measuring 0.10 cm × 0.16 cm × 0.21 cm. From mass and volume, we estimated a 5.059-g/cm^3 mass density, within about 0.5% of the x-ray density. For measurements, we used resonant-ultrasound spectroscopy [11].

For the C_{ij}, we found the results summarized in Table I. These give a (110) $[\bar{1}10]$ shear modulus $C' = (C_{11} - C_{12})/2 = 40.5$ GPa, a bulk modulus $B = (C_{11} + 2C_{12})/3 = 74.5$ GPa, and a Zener elastic anisotropy $A = C_{44}/C' = 0.677$. The 0.43% rms frequency measurement uncertainty means C_{ij} uncertainties of about 1%.

Figure 2 shows our results expressed as ratios $C_{ij}(T)/C_{ij}$ (300 K). Instead of C_{11}, C_{12}, and C_{44}, we show the more physical Zener elastic constants $C' = (C_{11} - C_{12})/2$, C_{44}, and $(C_{11} + 2C_{12})/3$, with the latter being the bulk modulus B. Because zirconium tungstate

TABLE I. Values of the monocrystal C_{ij} and the average-over-direction effective elastic constants: bulk modulus B, Young modulus E, shear modulus G, Poisson ratio ν, and Debye temperature calculated from the C_{ij}.

T (K)	C_{11} (GPa)	C_{12} (GPa)	C_{44} (GPa)	B (GPa)	E (GPa)	G (GPa)	ν	Θ_D
300	128.4	47.5	27.4	74.5	88.3	33.9	0.303	(321)
0	161.8	75.5	29.4	104.3	98.8	36.8	0.342	333

 0031-9007/04/93(2)/025502(4)$22.50

shows small elastic anisotropy, $C' = C_{44}$, for convenience we sometimes also invoke the shear modulus in Voigt's approximation, $G = (2C' + 3C_{44})/5$. Table I gives the monocrystal C_{ij}, the average-over-direction effective elastic constants, and the Debye temperature Θ_D calculated from the C_{ij}.

Compared with 17 other oxides [12], zirconium tungstate is relatively soft. Its bulk modulus B equals 53% of the average value. The effective shear modulus G is 44% of the average. (Here, we calculated G by Kröner's averaging method [13].) This relative softness reflects the crystal structure and the interatomic bonding. One view of zirconium tungstate's negative thermal expansion is that rigid ZrO_6 octahedra rotate toward or away from alignment with the unit-cell axes, altering the volume [14]. The softness to rotation appears in the bulk modulus, and more so in the shear modulus.

Our bulk-modulus result, $B = 74.5$ GPa, compares reasonably well with a high-pressure powder-specimen neutron-diffraction study: $B = 72.5$ GPa [9]. Both measurements refute a much-lower theoretical estimate [10]. A theoretical lattice-dynamics study [5] gave $B = 88.4$ GPa. This calculation included both ionic and covalent interatomic potentials. Below, we describe that our measured C_{ij} suggest a weak covalent component.

To characterize crystal elastic anisotropy, one usually invokes Zener's anisotropy definition [15]:

$$A = 2C_{44}/(C_{11} - C_{12}). \quad (1)$$

However, for materials with A less than unity (the present case), a better definition arises, as emphasized by Chung and Buessem [16]. These authors suggested

$$A^* = (G_V - G_R)/(G_V + G_R). \quad (2)$$

Here, G_V and G_R denote effective shear moduli calculated from the C_{ij} using Voigt or Reuss methods. For isotropic materials, $A^* = 0$. For a high-anisotropy material such as sodium, $A^* \approx 40$. For zirconium tungstate, $A^* = 0.02$, that is, nearly isotropic. With NiO and $BaTiO_3$ as exceptions, none of the oxides shown in Fig. 1 possess strong elastic anisotropy, and both exceptions are metastable.

Some studies [6] concluded that zirconium tungstate, because of its linkage crystal structure, may possess a negative Poisson ratio:

$$\upsilon_{ij} = -(S_{ij}/S_{ii}). \quad (3)$$

Here S_{ij} denotes the contracted S_{ijkl}tensor inverse of the C_{ijkl}. Because the material shows near elastic isotropy, we can consider the average-over-direction Poisson ratio, which relates to the bulk modulus B and effective shear modulus G:

$$\upsilon = (1/2)[(3B - 2G)/(3B + G)]. \quad (4)$$

The effective Poisson ratio equals 0.30, not only positive but also a value typifying many positive-thermal-expansion materials. Thus, although many linkage-structure materials show negative Poisson ratios, zirconium tungstate does not.

To learn something about the interatomic bonding, we use a Blackman diagram [17,18], Fig. 1. In such a diagram showing reduced C_{ij}, materials with similar bonding cluster. Figure 1 shows that zirconium tungstate falls among the oxides, on the low C_{44}/C_{11} side, away from covalent compounds, which fall more in the center [18]. This location suggests a strong ionic contribution, and a weaker covalent contribution. Some lattice-dynamics calculations included both contributions [5], which would predict a stiffer material. Also, some studies suggested that negative thermal expansion requires high covalency [19]. If so, this covalency fails to affect the elastic constants. The Poisson ratio (0.30), being much higher than the ≈ 0.20 covalent limit [20], also suggests strong ionicity. On bonding, finally we note the small-moderate departure from the Cauchy condition $C_{12} = C_{44}$, a departure usually taken to indicate noncentral-force bonding. Again ZrW_2O_8 behaves similar to a typical oxide.

Some authors suggested elastic instabilities [5]. In Fig. 1, the Born instability conditions occur as lines $C_{12}/C_{11} = 1$ and $C_{44}/C_{11} = 0$. On this diagram, points move only slightly in response to changes in composition, temperature, and pressure. Thus, the zirconium-tungstate point occurs well away from mechanical instability.

From the C_{ij}, we can calculate an elastic Debye temperature Θ. At zero temperature Θ_{elastic} equals $\Theta_{\text{specific-heat}}$ [21]. To calculate Θ, we use the relationship

$$\Theta = (h/k)(3/4\pi V_a)^{1/3}\upsilon_m. \quad (5)$$

Here, h and k take their usual meanings, V_a denotes

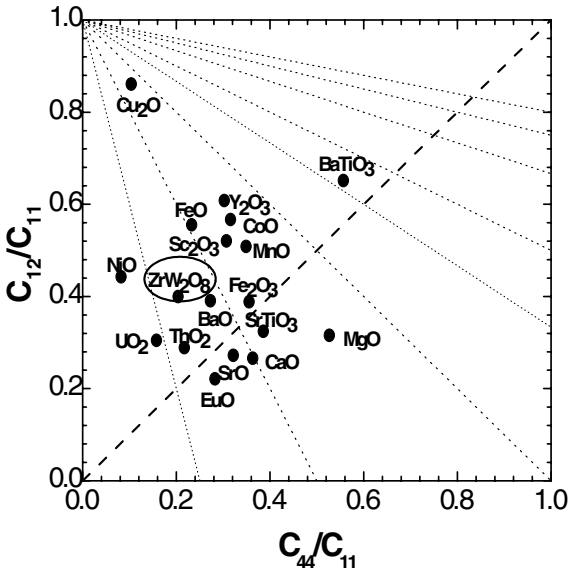

FIG. 1. Blackman diagram showing points for ZrW_2O_8 and seventeen other oxides. We see that ZrW_2O_8 looks normal.

atomic volume, and v_m denotes mean sound velocity, which we calculated from the C_{ij} using the Christoffel equations. For $T = 0$ K, we estimate $\Theta = 333 \pm 5$ K. Our result differs 7% from a recent specific-heat result: $\Theta = 311$ K [22].

Using the bulk modulus B, we can calculate the quintessential anharmonic-property parameter, the Grüneisen parameter:

$$\gamma = B_s \beta V / C_p. \tag{6}$$

Here β denotes volume thermal expansivity, V volume, and C_p heat capacity. For these properties we took $\beta = -26.4 \times 10^{-6}$ K^{-1}, V(unit cell) = 767.22 Å^3, $C_p = 207$ J K^{-1} mol^{-1}. Substitution gives the total thermodynamic (effective, average-over-mode) Grüneisen parameter $\gamma = -1.2$, consistent with several previous reports [3,22].

For a typical oxide such as CaO, in the temperature region 300 to 100 K, cooling increases the shear modulus about 5% and the bulk modulus about 4% [23]. From quasiharmonic-model thermodynamics, the bulk-modulus temperature derivative has the form [24]

$$(\partial B_S/\partial T)_P = -\delta_S \beta B_S = -(\gamma + 1)\beta B_S. \tag{7}$$

Here S denotes entropy, P pressure, δ the second Grüneisen parameter, β the thermal expansivity $(1/V)(\partial V/\partial T)_P$, and γ the usual (first) Grüneisen parameter. For typical materials where γ ranges from 1 to 3, the derivative is usually negative. Indeed the measured $\partial B/\partial T$ provides a way to estimate γ. For zirconium tungstate, γ is negative and β is negative. Thus, from Eq. (7) one expects a negative $\partial B/\partial T$. Deriving an expression for the shear-modulus temperature dependence requires more assumptions. As an example, using Born's central-force near-neighbor-only face-centered-cubic model gives [25]

$$(\partial G/\partial T)_P = (9/28)(\partial B/\partial T)_P. \tag{8}$$

Taking a typical Poisson ratio, $v = 1/3$, then $G/B = 3/8$, and we obtain

$$(B/G)(\partial G/\partial T)(\partial B/\partial T) = 6/7. \tag{9}$$

So, approximately, in Born's model the relative shear-modulus change with temperature equals the relative bulk-modulus change. Born's model may apply fairly well to zirconium tungstate because central-interatomic-force potentials enjoyed some success [5] and because the ZrO_6 octahedra occupy fcc lattice positions [26].

Figure 2 presents three major surprises: (i) All the elastic constants stiffen during cooling, against the expectation that they should soften because the volume increases and the bulk modulus varies with volume as $B \propto V^{-4/3}$. (ii) The shear-modulus increase agrees with that of a typical oxide. (iii) The bulk modulus changes differently from the shear modulus. Indeed the bulk modulus increases enormously. The 40% increase in the bulk modulus is unprecedented [27]. The increase breaks Birch's law of corresponding states: The bulk modulus depends on volume, not on how one changes volume—by temperature, pressure, composition, or phase transformation [28,29]. The Birch-law breakage provides strong evidence that the material's internal state changes during cooling. Another surprise is the near linearity to such low temperatures, or the low temperature at which the elastic constants begin to reflect strongly the zero-point energy. Also, we see unusual behavior in the Zener elastic anisotropy: $A = C_{44}/C'$ is essentially temperature invariant. Curiously, the bulk modulus extrapolates to zero near the material's decomposition temperature, 1050 K.

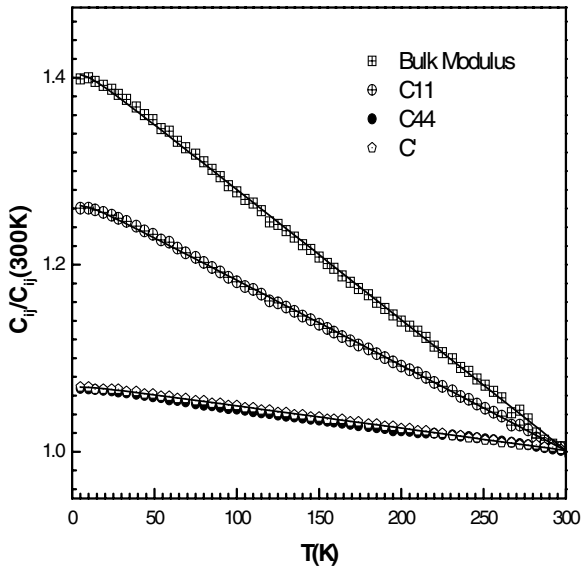

FIG. 2. Zirconium tungstate's normalized low-temperature elastic constants: bulk modulus B, C_{11}, C_{44}. Curves represent an Einstein-oscillator function. The bulk-modulus increase may be the largest ever reported. The near linearity to such low temperatures strongly suggests a low-frequency Einstein mode.

To the measurements in Fig. 2, we fit an expression based on the assumption that elastic stiffness decreases linearly with the thermal-oscillator-energy increase [30]:

$$C(T) = C_0 - s/(e^{t/T} - 1). \tag{10}$$

Here, C_0 denotes the zero-temperature elastic stiffness and t relates to the average Einstein temperature. Originally an adjustable parameter, in a quasiharmonic Einstein-oscillator model, s becomes [31]

$$s = C_h - C_0 = 3kt\gamma(\gamma + 1)/V_a. \tag{11}$$

Here C_h denotes the harmonic zero-temperature elastic constant obtained by linear extrapolation from high temperatures, k is the Boltzmann constant, γ is the Grüneisen parameter, and V_a is the atomic volume. The high-temperature slope follows as

TABLE II. Einstein temperature calculated by fitting Eq. (10) to the $C_{ij}(T)$.

C_{ij}	C_{11}	C_{12}	C_{44}	C'	B
Θ_E (K)	26	23	17	34	25

$$dC/dT = -3k\gamma(\gamma + 1)/V_a. \quad (12)$$

Solving this relationship for γ and taking the negative root gives $\gamma = -7.0$, which differs sharply from the ambient-temperature value of $\gamma = -1.2$, and heads toward the large negative low-temperature values reported from thermal-expansion and specific-heat measurements [3,22].

The results of fitting Eq. (10) to the C_{ij}, and taking t to be an Einstein temperature Θ_E are summarized in Table II. For zirconium tungstate $t = 25\ \mathrm{K} = 0.07\Theta_D$, enormously lower than expected.

The low values obtained for Θ_E reflect a dominant low-frequency acoustic-vibration mode. The lowest value of Θ_E appears for C_{44}, the (100) $[0kl]$ shear mode, and the highest Θ_E corresponds to $C' = (C_{11} - C_{12})/2$, the (110) $[\bar{1}10]$ shear mode. However, Θ_E shows remarkably low values for all modes, shear and dilational. These results agree with and confirm previous heat-capacity and phonon-density-of-states studies, which found low-frequency Einstein-type vibration modes.

Despite its peculiar anharmonic properties, zirconium tungstate possesses monocrystal elastic constants (harmonic properties) that present no surprises. Compared with other oxides, it is slightly soft, nearly isotropic, mechanically stable, and shows normal Poisson ratios. A Blackman diagram suggests strong ionic bonding. Its elastic-constant temperature derivatives (anharmonic properties) behave remarkably, perhaps uniquely, in both the magnitudes and the signs of the various dC_{ij}/dT. At a fundamental level, the C_{ij}-T behavior must relate to the remarkable negative-thermal-expansion behavior ZrW_2O_8; both depend on the Grüneisen parameter γ.

This research proceeded under the auspices of the National Science Foundation, the State of Florida, and the U.S. Department of Energy. J. Van Duijn also thanks DOE Grant No. DE-FG02-02ER45983 for support of this research.

[1] C. Martinek and F. Hummel, J. Am. Ceram. Soc. **51**, 227 (1968).
[2] A. P. Ramirez and G. R. Kowach, Phys. Rev. Lett. **80**, 22 (1998).
[3] G. Ernst, C. Broholm, G. Kowach, and A. Ramirez, Nature (London) **396**, 147 (1998).
[4] T. Ravindran, A. Arora, and T. Mary, Phys. Rev. B **67**, 064301 (2003).
[5] R. Mittal and S. Chaplot, Phys. Rev. B **60**, 7234 (1999).
[6] D. Cao, F. Bridges, and A. Ramirez, Phys. Rev. B **68**, 014303 (2003).
[7] J. Evans, W. David, and A. Sleight, Acta Crystallogr. Sect. B **55**, 333 (1999).
[8] A. Sleight, Curr. Opin. Solid State Mater. Sci. **3**, 128 (1998).
[9] J. Evans *et al.*, Science **275**, 61 (1997).
[10] A. Pryde *et al.*, J. Phys. Condens. Matter **8**, 10 973 (1996); N . Allan *et al.*, Phys. Chem. Phys. **2**, 1099 (2000) challenged the validity of the interatomic potential used in this study.
[11] A. Migliori and J. Sarrao, *Resonant Ultrasound Spectroscopy* (Wiley-Interscience, New York, 1997).
[12] H. Ledbetter and S. Kim, in *Handbook of Elastic Properties of Solids, Liquids, and Gases* (Academic, San Diego, 2001), Vol. II, p. 65.
[13] E. Kröner, Z. Phys. **151**, 504 (1958).
[14] A. Pryde *et al.*, Phase Transit. **61**, 141 (1997).
[15] C. Zener, *Elasticity and Anelasticity of Metals* (University of Chicago Press, Chicago, IL, 1948), p. 16.
[16] D. Chung and W. Buessem, J. Appl. Phys. **38**, 2010 (1967).
[17] M. Blackman, Proc. R. Soc. London **164**, 62 (1938).
[18] H. Ledbetter, *Handbook of Elastic Properties of Solids, Liquids, and Gases* [Ref. [12], p. 57].
[19] T. Mary, J. Evans, T. Vogt, and A. Sleight, Science **272**, 90 (1996).
[20] H. Ledbetter and S. Kim, *Handbook of Elastic Properties of Solids, Liquids, and Gases* [Ref. [12], p. 281].
[21] G. Leibfried and W. Ludwig, Solid State Phys. **12**, 275 (1961).
[22] Y. Yamamura *et al.*, Phys. Rev. B **66**, 014301 (2002).
[23] O. Anderson, *Equation of State of Solids* (Oxford, New York, 1995), p. 366.
[24] E. Grüneisen, in *Handbuch der Physik* (Springer-Verlag, Berlin, 1926), p. 1, Eq. (46).
[25] M. Gow, Proc. Cambridge Philos. Soc. **40**, 151 (1944).
[26] M. Auray, M. Quarton, and M. Leblanc, Acta Crystallogr. Sect. C **51**, 2210 (1995).
[27] A. Every and A. McCurty, in *Second and Higher Order Elastic Constants*, Landolt-Bornstein, New Series, Group III, Vol. 29a (Springer-Verlag, Berlin, 1992).
[28] F. Birch, J. Geophys. Res. **66**, 2199 (1961).
[29] F. Stacey, *Physics of the Earth* (Brookfield, Kenmore, Australia, 1992), p. 278.
[30] Y. Varshni, Phys. Rev. B **2**, 3952 (1970).
[31] H. Ledbetter, Phys. Status Solidi (b) **181**, 81 (1994).